Clinical Hemorheology and Microcirculation 27 (2002) 27–41
IOS Press

Towards a quantitative *in vivo* evaluation of venous blood echogenicity: Image processing versus subjective assessment

Yayha A. Rabhi [a], Pascale Fabbro-Peray [b], Michel Dauzat [a,*], Philippe Montesinos [c], Marie-Claire Oliva-Lauraire [a], François-Michel Lopez [d], Isabelle Quéré [e], Jean-Christophe Gris [a], Jean-Frédéric Brun [f] and Léandre Pourcelot [g]

[a] *Laboratory of Cardio-Vascular Physiology, Faculty of Medicine, Montpellier I University, Nimes, France*
[b] *Department of Epidemiology and Biostatistics, University Hospital Center, Nimes, France*
[c] *Computer Assisted Vision Laboratory LGI2P, EMA-EERIE, Nimes, France*
[d] *Medical Imaging Department, University Hospital Center, Nimes, France*
[e] *Department of Vascular Medicine, University Hospital Center, Montpellier, France*
[f] *Department of Clinical Physiology, University Hospital Center, Montpellier, France*
[g] *In vivo Nuclear Medicine and Ultrasound Laboratory, University Hospital Center, Tours, France*

Abstract. *Purpose*: Spontaneous blood echogenicity in vein ultrasound images may be a marker for an increased erythrocyte aggregability, but a reliable quantitative evaluation method is a prerequisite for its use in clinical studies. We compared a simple scoring system of blood echogenicity intensity and pattern, with automatic image analysis.

Material and methods: 157 femoral and popliteal vein digitized ultrasound sequences were reviewed by two independent observers who chose an image, delimited an area of interest (*ROI*), and graded blood echogenicity intensity and pattern, using a four class score. Each observer reviewed the images selected by the other, without and with *ROI*. The computer calculated first and second order parameters describing echo intensity and spatial organization.

Results: Inter-observer reproducibility of subjective assessment was poor (Kappa < 0.5), whereas the automatically calculated *ROI* average gray level intensity relatively to the whole image (τ_1) effectively separated all grades of intensity. No parameter effectively separated patterns.

Conclusion: τ_1 is a simple parameter for the *in vivo* evaluation of blood echogenicity intensity. It should be evaluated in standardized conditions for clinical hemorheology studies in correlation with *in vitro* erythrocyte aggregation measurements.

Keywords: Ultrasound, vein, blood, echogenicity, image analysis, computer

1. Introduction

Spontaneous echogenicity of the flowing blood is very commonly seen on B-mode ultrasound images of peripheral veins (often referred to as "spontaneous blood flow echogenicity") [1–3] as well as in the atrium and left atrium appendage during echocardiography examination (often referred to as "spontaneous echocardiographic contrast") [4–7].

Most authors acknowledge that spontaneous blood echogenicity is mostly related to blood stasis [8–10], facilitating red cell aggregation [11], modulated by plasma proteins [12–21]. Spontaneous

*Corresponding author: Professor Michel Dauzat, Laboratory of Cardio-Vascular Physiology, Faculty of Medicine, Avenue Kennedy, 30907, Nîmes, France. Tel.: +33 4 66 23 49 73; Fax: +33 4 66 23 55 38; E-mail: dauzat@sc.univ-montp1.fr.

echocardiographic contrast have been associated with a hypercoagulable state [22] and an increased rate of thromboembolic events [23–28].

In contrast with the large number of reports concerning spontaneous echocardiographic contrast and the thrombo-embolic risk it implies, very few studies have described and analyzed *in vivo* spontaneous blood echogenicity in peripheral vessels, although this is a very common finding. *In vitro* studies demonstrated greater blood echogenicity in patients with arterial claudication [29], or with suspected venous thrombosis [15]. *In vivo*, spontaneous blood echogenicity is commonly seen in the lower limb veins of healthy subjects when blood stasis is induced by the sitting position [9]. During uncomplicated pregnancy, increased lower limb vein diameter, together with a decrease in hematocrit and an increase in fibrinogen concentration, result in spontaneous blood echogenicity in the femoral veins, which has to be considered as a physiological phenomenon [3]. In the aorta, spontaneous blood echogenicity was found especially in older, male patients with a large aorta and complex atherosclerosis, and was associated with a high prevalence of embolic events [30].

In our clinical practice, spontaneous blood echogenicity is a very common phenomenon that we have to interpret in reference to the position and clinical status of the subject. In lower limb veins, blood stasis may be induced by any mechanical obstacle along the venous path (a venous thrombus as well as extrinsic compression by an aneurysm, hematoma, popliteal cyst, etc.) [31] or increased abdominal pressure. Therefore, spontaneous blood echogenicity may be a clue to the positive and differential diagnosis of venous thrombosis. On the other hand, when not explicable by stasis, spontaneous blood echogenicity may suggest some underlying rheological or hematological disorder, with increased thromboembolic risk. As blood stasis itself constitutes a risk factor for thrombosis, spontaneous blood echogenicity could be proposed as a marker of thromboembolic risk. Nevertheless, large prospective studies would be necessary to assess the exact significance of this phenomenon, and to validate its clinical use. A major drawback for the setup of such studies is that the level of blood echogenicity depends largely on machine settings, while its evaluation is highly operator dependent. Therefore, observation conditions have to be standardized, and an evaluation method has to be precisely defined and its reproducibility assessed before any prospective study can be planned and performed.

The ideal method for grading blood echogenicity should be both machine and operator independent. As there are many different ultrasound systems on the market, and as they are used in many different ways to obtain the same diagnostic information, standardization of image acquisition should be reduced to simple and universal recommendations. On the other hand, the scoring system should be detailed enough to allow the detection of minor changes in blood echogenicity during longitudinal or pharmacological studies.

The aim of our study was therefore to evaluate the reproducibility of a simple scoring system of blood echogenicity, and its comparison with automatic image analysis by first and second order parameters describing echo intensity and spatial organization.

2. Material and methods

During lower limb vein ultrasound examination of patients referred to the Vascular Laboratories of the two participating University Hospitals for suspicion of deep venous thrombosis, video sequences were routinely stored on a computer for subsequent review and archiving. An anonymous thesaurus of femoral and popliteal vein video sequences was constituted from these archives.

Lower limb vein examinations were conducted by several medical doctors following the same protocol. The patient was lying supine on a strictly horizontal bed, at rest and breathing normally. B-mode

ultrasound sequences were acquired with Acuson 128 XP or Aspen systems (Acuson, Mountain View, CA) with a 7.5 linear array probe. The machine settings were initially identical (peripheral vein preset), but could be freely altered when necessary, depending on the vein depth and overall echogenicity.

The Y/C video signal was digitized via the built-in video frame grabber and sequences were stored as movies on a Macintosh 8500/180 PowerPC computer. Image processing and analysis was then performed independently, with IÔ 3.1 software (IÔDP, Paris) and a dedicated analysis and calculation software module developed in the laboratory.

Two independent observers read each sequence, selected one or several representative images (provided that images from the same patient corresponded to different veins or different parts of a vein, so that there was no duplicate), drew the area or "region of interest" (*ROI*) perimeter around the representative part of the B-mode image *I* (i.e. the part of the vein lumen showing spontaneous blood echogenicity, if any, or the greater artifact free part of the vein lumen when no blood echogenicity could be seen), and subjectively evaluated the intensity and spatial organization of blood echogenicity (Fig. 1). Each observer was blinded from the patient's identity and clinical status, as well as from the other observer's assessment and from calculation results of the software module. Both observers were medical doctors, with more than 2 years' (B) or 20 years' (A) experience of vascular sonography. They reviewed together twenty studies before starting the project.

The analysis was performed in three steps: (1) Observer A read each movie, selected freely one or several representative images, drew freely the *ROI*, and subjectively evaluated blood echogenicity. Observer B did the same, independently. Images and *ROIs* selected by each observer were stored. (2) Ob-

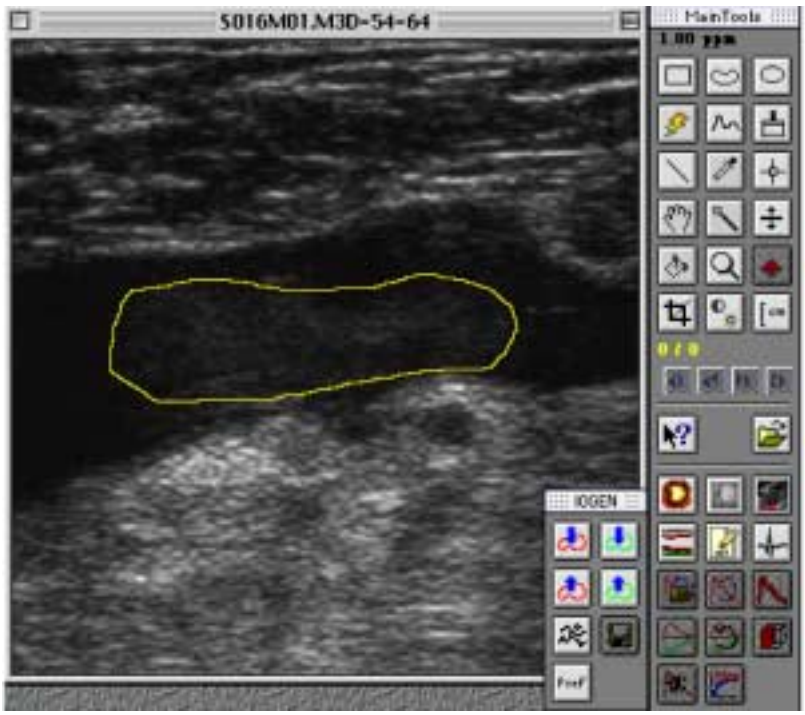

Fig. 1. Example of femoral vein ultrasound image with the ROI encircling the area in which the observer detected spontaneous blood echogenicity. Anonymous sequence and image identification appears on the top of the screen, while software tools appear on the right side.

server A read each image selected by observer B (without observer B's *ROI*), drew freely his own *ROI*, and subjectively evaluated blood echogenicity. Observer B did the same with images selected by observer A. (3) Observer A subjectively evaluated blood echogenicity of each image selected with *ROI* drawn by observer B. Observer B did the same with images selected with *ROIs* drawn by observer A. At step 1 and 2, the computer software module calculated two sets of parameters characterizing blood echogenicity in the *ROI*.

2.1. Subjective evaluation and grading by two independent observers

Subjective grading of the intensity of spontaneous blood echogenicity on B-mode ultrasound images of peripheral veins was performed according to the following scale [3]: grade 0, anechoic (no echo visible in the lumen); grade 1, barely visible echoes in the lumen; grade 2, clearly visible echoes whose intensity remained lower than that of surrounding tissues; grade 3, blood echogenicity equal to or greater than the echogenicity of surrounding tissues.

The pattern of blood echogenicity was subjectively assessed in order to differentiate the swirling echogenicity of flowing blood, commonly described as "smoke", from echogenic clumps or filaments. Classification was as follows: 1, homogeneous echogenicity; 2, echogenic clumps or filaments; 3, mixed echogenicity pattern.

2.2. Objective image processing and analysis by computer software

Image analysis was performed in the *ROI* drawn by the observer by a dedicated software module including user interface and calculation algorithms, written in C programming language with CodeWarrior V3.0 integrated development environment (Metrowerks, Austin, TX). This software automatically calculated two sets of first and second order parameters [32,33] describing the absolute and relative gray level intensity of echoes in the *ROI*, as well as the spatial organization of spontaneous blood echogenicity, if any.

With N_I the total number of pixels in the whole image I; N_{ROI} the number of pixels in the *ROI*; $\overline{ROI} = I - ROI$; $N_{\overline{ROI}}$ the number of pixels in $\overline{ROI}$, and $I_{(i,j)}$ the gray level intensity of a given pixel whose coordinates are i and j; a first set of parameters was calculated to describe the gray level intensity or "echogenicity":

Average gray level intensity of the *ROI*

$$m_{ROI} = \frac{1}{N_{ROI}} \sum_{k=1}^{N_{ROI}} I_{(i,j)}. \tag{1}$$

Average gray level intensity outside the *ROI*

$$m_{\overline{ROI}} = \frac{1}{N_{\overline{ROI}}} \sum_{k=1}^{N_{\overline{ROI}}} I_{(i,j)}. \tag{2}$$

Average gray level intensity of the whole image

$$m_I = \frac{1}{N_I} \sum_{k=1}^{N_I} I_{(i,j)}. \tag{3}$$

Average gray level intensity of the *ROI* relative to the whole image

$$\tau_1 = \frac{m_{ROI}}{m_I}. \tag{4}$$

Average gray level intensity of the *ROI* relatively to the image outside the *ROI*

$$\tau_2 = \frac{m_{ROI}}{m_{\overline{ROI}}}. \tag{5}$$

Local variance of gray level intensity in the *ROI* (a smooth image has a small variance)

$$\sigma^2 = \frac{1}{N_{ROI}} \sum_{k=1}^{N_{ROI}} (I(i,j) - m_{ROI})^2. \tag{6}$$

Skewness of *ROI*, measuring the asymmetry of the frequency distribution histogram of pixels gray levels

$$ske = \frac{1}{N_{ROI}} \sum_{k=1}^{N_{ROI}} \left(\frac{(I(i,j) - m)}{\sigma} \right)^3. \tag{7}$$

Kurtosis of *ROI*, indicating the flatness of the histogram

$$kur = \frac{1}{N_{ROI}} \sum_{k=1}^{N_{ROI}} \left(\frac{(I(i,j) - m)}{\sigma} \right)^4. \tag{8}$$

Regional Entropy of *ROI*, describing the image detail and clutter

$$Ent_R = -\frac{1}{N_{ROI}} \sum_{k=1}^{N} I(i,j) \ln I(i,j) 1_{I(i,j)} \tag{9}$$

with $(i,j) \in R$ and $1_{I(i,j)} = 1$ if $I(i,j) \neq 0$ and $1_{I(i,j)} = 0$ if $I(i,j) = 0$.

Kolmogorov–Smirnov test of *ROI*, measuring image homogeneity $KS(H, H_0)$ (see Appendix A).

The co-occurrence matrix [34,35] (see Appendix B) was used for the calculation of a set of second order parameters (see Appendix C), relative to the spatial organization and texture of the *ROI* [32,36], with $\theta = 0^\circ$ and 90°, and $d = 1$, because these values are commonly used for the analysis of ultrasound images [35]. This set of parameters included contrast ($CON_{\theta,d}$) as a measure of the variation in intensity between pixels, energy ($ENE_{\theta,d}$) as a measure of global image homogeneity, local homogeneity ($HOGL_{\theta,d}$), directional entropy ($ENTD_{\theta,d}$) as a measure of image disorder, correlation ($COR_{\theta,d}$) as a measure of correlation between two pixels, and *KAP* ($KAP_{\theta,d}$), as a measure of periodicity in the image [35]. The software calculated also $\overline{CON}$, $\overline{ENE}$, $\overline{HOGL}$, $\overline{ENTD}$, $\overline{COR}$, and $\overline{KAP}$ as the mean values of these parameters with $\theta = 0^\circ$, 45°, 90°, and 135°, and $d = 1$ (for example: $\overline{CON} = (CON_{0,1} + CON_{45,1} + CON_{90,1} + CON_{135,1})/4$.

2.3. Statistical analysis

The statistical analysis was performed with SAS V6.06 software (SAS Institute Inc, 1987 Cary, NC). Agreement between observers was assessed by the Kappa test while disagreement between observers was assessed by McNemar's test, for each intensity grade and pattern of blood echogenicity, and each class of image quality, separately and after pooling. For each subjective parameter and each observer, analysis of variance was performed to compare the calculated parameters for each of the observer's grades. When analysis of variance showed significant differences between groups, the Newman–Keuls post-test was used to identify the differences between the grades. Inter-observer differences in calculated parameters at step 1 and 2 were evaluated by the Student's t test for paired data. Correlation between parameters calculated at step 1 and step 2 for observer A and observer B was evaluated by Pearson's parametric and Spearman's non-parametric correlation coefficients.

Multivariate analysis using the logistic model was performed to explain each subjective parameter by the most informative calculated parameters. For each set of calculated parameters, an unconditional logistic regression was performed to select the most informative variables, that were introduced into a global multivariate logistic model to control for all the confounding calculated parameters, as described by Hosmer and Lemeshow [37]. For model building, we have applied forward stepwise introduction of variables (p-entry 0.05). Results were considered as significant when $p < 0.05$.

3. Results

From 157 examination sequences of 75 patients, observer A selected and analyzed 193 images, whereas observer B selected 136 images (step 1).

At step 2, observer A read the 136 images selected by observer B and drew and analyzed 142 *ROIs*, while observer B read the 193 images selected by observer A and drew and analyzed 196 *ROIs* (in some instances, the observer read the same image twice and drew different *ROIs*). At step 3, observer A analyzed 143 images selected with *ROIs* drawn by observer B (one image was read twice), while observer B analyzed 173 images selected with *ROIs* drawn by observer A (20 images were not read). Each *ROI* included at least 1000 pixels.

3.1. Inter-observer reproducibility of subjective assessment

Inter-observer reproducibility for intensity of spontaneous blood echogenicity evaluation was poor (Kappa < 0.5) except when grade 1, 2, and 3 were pooled and compared to grade 0 at step 1 (Kappa $= 0.57$, $p < 0.001$), at step 2 (Kappa $= 0.57$, $p < 0.001$), and at step 3 (Kappa $= 0.7$, $p < 0.001$). For the pattern of blood echogenicity, inter-observer reproducibility was poor at each step and for any pooling method.

3.2. Blood echogenicity intensity and calculated parameters

For observer A, τ_1 (Fig. 2), τ_2, m_{ROI}, σ^2, $KS(H, H_0)$, $HOGL_{0,1}$, ENT_R, and $CORL_{0,1}$ reliably separated all grades of blood echogenicity intensity. Some parameters (*ske*, *kur*, $ENE_{0,1}$, $HOM_{90,1}$, $CORL_{90,1}$, $\overline{COR}$) separated grade 0 from grade 1, 2, or 3 (but not grades 1, 2, and 3 from each other). Other parameters ($KAP_{0,1}$, $HOGL_{90,1}$, $ENTD_{90,1}$, $KAP_{90,1}$, $\overline{CON}$, $\overline{ENE}$, $\overline{HOGL}$, $\overline{ENTD}$, $\overline{COR}$, and $\overline{KAP}$) separated grade 0

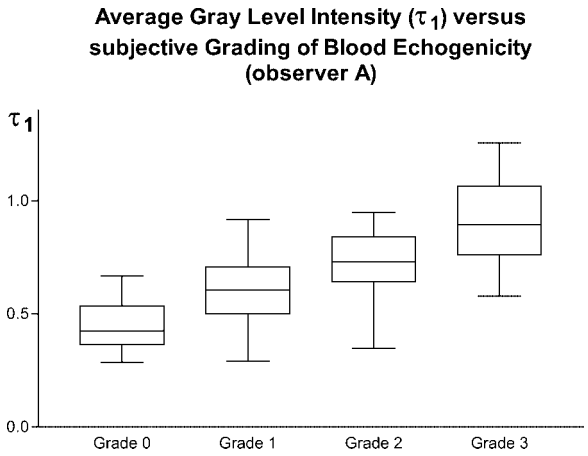

Fig. 2. Box and whiskers plot of the average gray level intensity of the region of interest relatively to the whole image (τ_1) versus subjective grading of spontaneous blood echogenicity intensity by observer A. The boxes extend from the 25th to the 75th percentiles, with the 50th percentile (median) as a horizontal line. The "whiskers" show the range of the data.

from grade 1 and from grades 2 or 3 but not grades 2 and 3 from each other. One parameter ($CON_{90,1}$) separated grades 0 or 1 from grades 2 or 3 but neither grade 0 from grade 1 nor grade 2 from grade 3.

For observer B, $KAP_{0,1}$ separated grade 0 or 1 from grade 2 or 3 but not grade 0 and 1 from each other. $\overline{CON}$ and $\overline{HOGL}$ separated only grade 0 from grade 3. $\overline{COR}$ separated only grade 0 from grade 2. $CON_{90,1}$ and $COR_{90,1}$ could not separate any grade. All other parameters separated grade 0 from grades 1, 2, or 3, but not grades 1, 2, and 3 from each other.

The Pearson parametric correlation coefficient for τ_1 was 0.8 ($p < 0.0001$) at step 1 and 0.8 ($p < 0.0001$) at step 2. The Spearman correlation coefficient for τ_1 was 0.9 ($p < 0.0001$) at step 1, and 0.84 ($p < 0.0001$) at step 2.

Multivariate analysis of observer A's results identified τ_1 ($p = 0.0023$) and σ^2 ($p = 0$) as the only independent parameters separating grade 0 or 1 from grade 2 or 3, with a 89.1% concordance rate. There was no significant difference in τ_1 ($p = 0.65$ and 0.43) and in σ^2 ($p = 0.97$ and 0.88) between *ROIs* selected by observer A and observer B, respectively on the same sequences (step 1) and on the same images (step 2).

3.3. Blood echogenicity pattern and calculated parameters

Pattern 2 was recognized in 9 cases by observer A, and in 16 cases by observer B. For observer A, *ENTR* separated pattern 2 from pattern 3, while $CON_{90,1}$, *CON*, and *HOML* separated pattern 2 from patterns 1 or 3, but not pattern 1 from pattern 3. For observer B, τ_1 and τ_2 separated all patterns, while m_{ROI}, $HOML_{0,1}$, $CON_{90,0}$, $HOML_{90,0}$, $\overline{CON}$ and $\overline{ENE}$ separated pattern 2 from pattern 1 or 3, but not pattern 1 from pattern 3. Pattern 2 and 3 were separated by σ^2, $ENTD_{0,1}$ and $\overline{KAP}$, whereas pattern 1 was separated from pattern 3 by $COR_{0,1}$ and from pattern 2 by $\overline{COR}$.

4. Discussion

On the basis of *in vitro* [38], and *in vivo* [39] studies, protein mediated erythrocyte aggregation appears to be the main mechanism of spontaneous blood echogenicity. *In vitro* studies showed that hematocrit

affected the rate of cell aggregation while fibrinogen controlled aggregate size and acoustic concentration [19]. Clinical studies confirmed the role of hematocrit, plasma viscosity, fibrinogen and plasma paraproteins [20,21]. The intensity of blood echogenicity results, on one hand, from technical factors (especially ultrasound frequency and signal processing), and, on the other hand, from several biological factors (hematocrit, flow velocity, turbulence, pulsatility, and fibrinogen concentration) that determine erythrocyte aggregation [40]. The relationship between hematocrit and ultrasound backscattering by blood is complex: backscattering increases with hematocrit at low hematocrit values, then decreases [41,43]. Shear rate and red cell aggregation alter this relationship in a complex way [44]. As the backscattered ultrasonic intensity depends on the size of erythrocyte aggregates [41,45], B-mode ultrasound has been used for *in vitro* evaluation of red cell [46] and platelet aggregation [47], and backscatter intensity is thought to provide an objective, quantitative method for the evaluation of blood echogenicity [48,49].

Semi-quantitative methods have been used for the grading of blood echogenicity and echocardiographic contrast on B-mode ultrasound images [21,50,51]. Only one study assessed the inter-observer variability of subjective spontaneous echo-contrast detection, and reported low variability [52], but we found no paper in the literature assessing the reproducibility and reliability of a scoring system. Quantitative video-densitometry was used by Fatkin et al. for the evaluation of spontaneous contrast on echocardiographic images [38], and for the evaluation of red cell aggregation in forearm subcutaneous veins by Kitamura et al. [39], but we found no data regarding the inter and intra-observer reproducibility of such techniques. Automatic analysis of B-mode ultrasound images by a set of first and second-order parameters have been used and validated for the characterization of carotid plaques [53], but has not been used so far for the evaluation of blood echogenicity.

In order to mimic the actual conditions of routine ultrasound vein examination, we designed a protocol allowing two independent observers to read and interpret the same ultrasound sequences, select the representative images, and delimit the part of the lumen showing spontaneous blood echogenicity, as if they were performing separately the examination of the same patient. The only limitation was that these sequences came from the same ultrasound device and were acquired with the same machine settings. Thus, our study could focus on subjective image interpretation and automatic image analysis, independently of technical parameters.

This study demonstrated that inter-observer reproducibility of the subjective assessment of blood echogenicity intensity and pattern is poor, except when observers are simply asked to answer by yes or no as for the presence of spontaneous blood echogenicity. Recent studies [54,55], yielded moderate to good agreement and demonstrated that reproducible grading of carotid plaque morphology was not consistently achievable, even by experienced observers, although inter-observer variability could be reduced by using binary classification [55]. In various fields, clinical studies demonstrated the relative inaccuracy of gray level perception [56]. No prospective clinical study is therefore possible on the sole basis of subjective grading, and a quantitative or semi-quantitative objective method is mandatory.

From the large sample of calculated parameters we tested, τ_1 (average gray level intensity of the *ROI* relatively to the whole image) and σ^2 (local variance of gray level intensity in the *ROI*) were the main independent parameters reliably describing the intensity of blood echogenicity in concordance with observer A, and without significant difference between observers when they drew freely and independently a region of interest on the same sequence or on the same image. Nevertheless, its interpretation will have to remain cautious, because the relationship between the size of red cell aggregates and the intensity of blood echogenicity is neither linear nor explicit [57].

Various parameters have been used for B-mode ultrasound image characterization of carotid plaque, but we found no data in the literature regarding their use for the quantification of blood echogenicity. Some authors used the median of the gray scale [58,59] as well as homogeneity, entropy, and contrast, for the evaluation of carotid plaques, and found that the median was a good predictor of hemispheric symptoms [60,61]. Other authors found the normalized mean gray level to be the most effective first-order parameter for the description of carotid plaque morphology [53]. Second order parameters were used with no definitive results by Tanzi et al. for the study of the neonatal heart [62].

As for blood echogenicity patterns, class 2 (echogenic clumps or filaments) was separated from class 1 (homogenous blood echogenicity) or class 3 (mixed pattern) for both observers by $CON_{90,1}$ (contrast for 90°), $\overline{CON}$ (mean contrast value), and $\overline{ENE}$ (energy). Indeed, the relatively small number of cases in class 2 do not allow to validate definitely these parameters for this application. Second order parameters could not help differentiating blood echogenicity patterns, probably because spontaneous blood echogenicity showed no typical texture.

Recent ultrasound systems offer a remarkably large dynamic range, so that blood echogenicity may become visible in most vessels when increasing gain. Conversely, reducing the dynamic range may result in the disappearance of blood echogenicity. Gain and TGC settings may also alter the level of echogenicity. Blickstein et al. demonstrated that manipulation of image parameters by computed sonographic technology obviates accurate echogenicity assessment [63], so that precise and standardized setting of the B-mode ultrasound machine is a prerequisite for image characterization and quantification [64], although normalization reduces the machine and gains dependence [65]. Therefore, standardization of machine settings and image acquisition procedure is essential before any computer assisted diagnostic method can be used for multicentric, prospective studies, especially when different duplex scanning systems and ultrasound probes are to be used. Such standardization may be achieved by zooming on the relevant area, using the maximum dynamic range, with linear postprocessing curve, and using a standard procedure for the setting of the overall gain and TGC [66]. Stored images may also be normalized by algebraic scaling with reference to normally anechogenic and hyperechogenic anatomical structures, as the carotid lumen and adventicia for the study of carotid plaques [66], or by dynamic range adjustment when no reliable reference structure can be found, as it is the case in most studies of veins, because blood echogenicity precludes the use of the vessel lumen as a zero reference level. In our study, the physicians in charge of collecting video sequences shared a common background and training, so that they used to set the sonographic system in the same way, especially as regards overall gain and TGC. Nevertheless, they remained free to alter these settings in order to obtain the best image whenever technical or anatomical problems were encountered, because we felt that more strict rules could not be imposed in the clinical practice for multicentric studies involving different observers, different machines, and different conditions. We reduced the effects of machine settings by calculating relative parameters, and it is therefore quite demonstrative that the most effective parameter for the evaluation of blood echogenicity intensity was τ_1, the average gray level intensity of the region of interest relatively to the whole image.

On the other hand, the cooccurrence matrix parameters depend on the number of diffuse scatterers and on the speckle size, which, in turn, is depth dependent, especially with sector scanning ultrasound probes [35]. We minimized this problem by using only linear probes, with the same transmitting frequency, and on a limited area (*ROI*).

Another potentially confounding variable is blood velocity, since red cell aggregation depends on shear stresses. Spontaneous blood echogenicity may be expected to occur more frequently in large veins with low flow velocity. Patients were examined in the same, resting conditions, but individual differences may

blur the threshold between normal and abnormal situations. This problem did not preclude the demonstration of spontaneous echocardiographic contrast as a risk marker for thrombosis, since blood echogenicity in the atrium is, almost always, an abnormal finding. On the contrary, spontaneous blood echogenicity in peripheral veins may be a perfectly normal finding in a healthy subject when blood stasis is created by posture or downstream compression. Therefore, models describing the *in vivo* relationship between flow velocity, vessel diameter, and red cell aggregation should be used to standardize the ultrasound examination in future clinical studies.

5. Conclusion

The average gray level intensity of the region of interest relatively to the whole image (τ_1) may be used as a simple and easily calculated parameter for the automatic, objective evaluation of the intensity of spontaneous blood echogenicity, to provide a non invasive marker of *in vivo* erythrocyte aggregability. This parameter has still to be validated by large prospective studies, before its clinical significance can be evaluated. At this stage, the technical conditions of image acquisition will have to be checked and, when possible, standardized, while physiological conditions will have to be, as far as possible, carefully controlled. As for the analysis of the echogenicity pattern, additional research, with the use of image filtering techniques, validated on a larger scale, would be necessary before this characteristic can be reliably assessed and used in clinical studies.

Acknowledgements

This work was supported by a French State grant from the Délégation Régionale à la Recherche et à la Technologie (1997–1998). We thank Souheil Mansour (IÔDP, Paris, France) for his help in software design and editing. We thank Frédérique Vivens, MD, Patricia Ponsi, MD, Bénédicte Fada, MD, and Catherine Charria, MD, for their help in data collection and interpretation. We thank Margaret Manson for her help in manuscript revision.

Appendix A: Kolmogorov–Smirnov test calculation

The histogram H of I is a vector of dimension *Lg*, defined as:

$$H = \{H(I, e),\ e = 0, 1, \ldots, Lg - 1\}, \tag{A.1}$$

where $H(I, e)$ is the number of pixels whose gray level is e, and *Lg* is the maximum gray level intensity of I, so that a set of *Lg* different (distinguished) histograms can be obtained. The distinguished (or minimal) histogram H_0 is a histogram where all gray levels (from 0 to *Lg*) are evenly represented:

$$H_0 = \left\{H(I, e) = \frac{Ir \times Ic}{Lg},\ e = 0, 1, \ldots, Lg - 1\right\}, \tag{A.2}$$

where *Ir* and *Ic* are respectively the number of raws and columns in I.

The Kolmogorov–Smirnov test of the minimal histogram is the distance between the image histogram and minimal histogram:

$$KS(H, H_0) = \sum_{0}^{Lg-1} \big(H(I, e) - H_0(I, e)\big). \tag{A.3}$$

Appendix B: Co-occurrence matrix

The co-occurrence matrix is a 2D histogram that describes the occurrence of pairs of pixels separated by a distance d in direction θ. For 2 pixels located respectively at the coordinates (i_1, j_1) and (i_2, j_2) with gray levels respectively $I(i_1, j_1)$, ($I(i_1, j_1) = x$) and $I(i_2, j_2)$, ($I(i_2, j_2) = y$), the normalized co-occurrence matrix $M\_C_{\theta,d}$ is:

$$M\_C_{\theta,d}(x, y) = Card \left\{ \begin{array}{l} ((i_1, j_1), (i_2, j_2)) \in I \times I / i_2 - i_1 = d * \sin\theta,\ j_2 - j_1 = d * \cos\theta \\ I(i_1, j_1) = x,\ I(i_2, j_2) = y \end{array} \right\} \Big/ N, \tag{B.1}$$

where *Card* is the number of elements in the set and N is the total number of pairs of pixels.

Appendix C: Second order parameters

The parameters contrast ($CON_{\theta,d}$), energy ($ENE_{\theta,d}$), local homogeneity ($HOGL_{\theta,d}$), directional entropy ($ENTD_{\theta,d}$), correlation ($COR_{\theta,d}$), and *KAP* ($KAP_{\theta,d}$) are defined by the following expressions:

$$CON_{\theta,d} = \sum_{x=0}^{Lg-1} \sum_{y=0}^{Lg-1} (x - y)^2 M\_C_{\theta,d}(x, y), \tag{C.1}$$

$$ENE_{\theta,d} = \sum_{x=0}^{Lg-1} \sum_{y=0}^{Lg-1} \big(M\_C_{\theta,d}(x, y)\big)^2, \tag{C.2}$$

$$HOGL_{\theta,d} = \sum_{x=0}^{Lg-1} \sum_{y=0}^{Lg-1} \frac{1}{1 + (x\_y)^2} M\_C_{\theta,d}(x, y), \tag{C.3}$$

$$ENTD_{\theta,d} = -\sum_{x=0}^{Lg-1} \sum_{y=0}^{Lg-1} M\_C_{\theta,d}(x, y) \ln M\_C_{\theta,d}(x, y) 1_{M\_C_{\theta,d}(x,y)}, \tag{C.4a}$$

where

$$1_{M\_C_{\theta,d}(x,y)} = 1 \quad \text{if } M\_C_{\theta,d}(x, y) \neq 0 \text{ and 0 else}, \tag{C.4b}$$

$$CORL_{\theta,d} = \frac{1}{\sqrt{\sigma_x^2 \sigma_y^2}} \sum_{x=0}^{Lg-1} \sum_{y=0}^{Lg-1} (x - \mu_x)(y - \mu_y) M\_C_{\theta,d}(x, y) \tag{C.5a}$$

with

$$\mu_x = \sum_{x=0}^{Lg-1} x \sum_{y=0}^{Lg-1} Mc(x, y) \tag{C.5b}$$

and

$$\sigma_x^2 = \sum_{x=0}^{Lg-1} (x - \mu_x) \sum_{y=0}^{Lg-1} Mc(x, y), \tag{C.5c}$$

$$KAP_{\theta,d} = \frac{P_0 - P_c}{P_m - P_c} \tag{C.6a}$$

with

$$P_0 = \sum_{x=0}^{Lg-1} M\_C_{\theta,d}(x, x), \tag{C.6b}$$

$$P_c = \sum_{x=0}^{Lg-1} \sum_{y=0}^{Lg-1} M\_C_{\theta,d}(x, y) M\_C_{\theta,d}(y, x), \tag{C.6c}$$

$$P_m = \sum_{x=0}^{Lg-1} \min\left\{ \sum_{y=0}^{Lg-1} M\_C_{\theta,d}(x, y), \sum_{y=0}^{Lg-1} M\_C_{\theta,d}(y, x) \right\}. \tag{C.6d}$$

References

[1] M.K. Wolverson, S. Nouri, J.H. Joist, M. Sundaram and E. Heiberg, The direct visualization of blood flow by real-time ultrasound: clinical observations and underlying mechanisms, *Radiology* **140** (1981), 443–448.

[2] R.S. Meltzer, V. Klig, C.A. Visser and L.E. Teichholz, Spontaneous echographic contrast in the inferior vena cava, *Am. Heart J.* **110** (1985), 826–830.

[3] Y. Rabhi, C. Charras-Arthapignet, J.C. Gris, J. Ayoub, J.F. Brun, F.M. Lopez, C. Janbon, P. Mares and M. Dauzat, Lower limb vein enlargement and spontaneous blood flow echogenicity are normal sonographic findings during pregnancy, *J. Clin. Ultrasound* **28** (2000), 407–413.

[4] H. Schuchman, H. Feigenbaum, J.C. Dillon and S. Chang, Intracavitary echoes in patients with mitral prosthetic valves, *J. Clin. Ultrasound* **3** (1975), 107–110.

[5] C. Wanishsawad, C. Roongsritong, C. Sitthi-Amorn and W. Puavilai, Spontaneous echo contrast on transthoracic echocardiography and left atrial thrombus in rheumatic mitral valve disease patients: a clinicopathologic study, *Clin. Cardiol.* **17** (1994), 547–551.

[6] R. Castello and S. Puri, In vivo and in vitro studies on the mechanism and clinical significance of spontaneous echocardiographic contrast in patients with atrial dysrhythmias, *Prog. Cardiovasc. Dis.* **39** (1996), 47–56.

[7] T.M. Lee, S.F. Su, K.L. Chien, Y.J. Lin, W.J. Chen, M.F. Chen, C.S. Liau and Y.T. Lee, Left atrial spontaneous echo contrast in patients with permanent pacemakers, *Heart* **78** (1997), 262–267.

[8] G.S. Reeder, J.E. Charlesworth and S.B. Moore, Cause of spontaneous echocardiographic contrast as assessed by scanning electron microscopy, *J. Am. Soc. Echocardiogr.* **7** (1994), 169–173.
[9] K. Kroger and G. Rudofsky, Duplex sonography of venous stasis, *Angiology* **48** (1997), 523–527.
[10] D. Fatkin, P. Roy, A. Sindone and M. Feneley, Rapid onset and dissipation of left atrial spontaneous echo contrast during percutaneous balloon mitral valvotomy, *Am. Heart J.* **135** (1998), 609–613.
[11] R.E. Shehada, R.S. Cobbold and L.Y. Mo, Aggregation effects in whole blood: influence of time and shear rate measured using ultrasound, *Biorheology* **31** (1994), 115–135.
[12] B. Sigel, J.C. Coelho, S.G. Schade, J. Justin and D.G. Spigos, Effect of plasma proteins and temperature on echogenicity of blood, *Invest. Radiol.* **17** (1982), 29–33.
[13] Y.W. Yuan and K.K. Shung, Ultrasonic backscatter from flowing whole blood. I: Dependence on shear rate and hematocrit, *J. Acoust. Soc. Am.* **84** (1988), 52–58.
[14] Y.W. Yuan and K.K. Shung, Ultrasonic backscatter from flowing whole blood. II: Dependence on frequency and fibrinogen concentration, *J. Acoust. Soc. Am.* **84** (1988), 1195–1200.
[15] A. Alanen, T. Kallio, I. Lehto and N. Wiernsperger, The effect of naftidrofuryl on red blood cell aggregation detected in vitro with ultrasound, *J. Cardiovasc. Pharmacol.* **16**(Suppl. 3) (1990), S33–S35.
[16] A. Merino, P. Hauptman, L. Badimon, J.J. Badimon, M. Cohen, V. Fuster and M. Goldman, Echocardiographic "smoke" is produced by an interaction of erythrocytes and plasma proteins modulated by shear forces, *J. Am. Coll. Cardiol.* **20** (1992), 1661–1668.
[17] X.F. Wang, L. Liu, T.O. Cheng, Z.A. Li, Y.B. Deng and J.E. Wang, The relationship between intracardiovascular smoke-like echo and erythrocyte rouleaux formation, *Am. Heart J.* **124** (1992), 961–965.
[18] E.G. Yamada, P.J. Fitzgerald, K. Sudhir, V.K. Hargrave and P.G. Yock, Intravascular ultrasound imaging of blood: the effect of hematocrit and flow on backscatter, *J. Am. Soc. Echocardiogr.* **5** (1992), 385–392.
[19] H. Kitamura, B. Sigel, J. Machi, E.J. Feleppa, J. Sokil-Melgar, A. Kalisz and J. Justin, Roles of hematocrit and fibrinogen in red cell aggregation determined by ultrasonic scattering properties, *Ultrasound Med. Biol.* **21** (1995), 827–832.
[20] I.W. Black, C.N. Chesterman, A.P. Hopkins, L.C. Lee, B.H. Chong and W.F. Walsh, Hematologic correlates of left atrial spontaneous echo contrast and thromboembolism in nonvalvular atrial fibrillation, *J. Am. Coll. Cardiol.* **21** (1993), 451–457.
[21] D.P. Briley, G.D. Giraud, N.B. Beamer, E.M. Spear, S.E. Grauer, J.M. Edwards, W.M. Clark, G.J. Sexton and B.M. Coull, Spontaneous echo contrast and hemorheologic abnormalities in cerebrovascular disease, *Stroke* **25** (1994), 1564–1569.
[22] L.M. Tsai, J.H. Chen and C.J. Tsao, Relation of left atrial spontaneous echo contrast with prethrombotic state in atrial fibrillation associated with systemic hypertension, idiopathic dilated cardiomyopathy, or no identifiable cause (lone), *Am. J. Cardiol.* **81** (1998), 1249–1252.
[23] M.I. Chimowitz, M.A. DeGeorgia, R.M. Poole, A. Hepner and W.M. Armstrong, Left atrial spontaneous echo contrast is highly associated with previous stroke in patients with atrial fibrillation or mitral stenosis, *Stroke* **24** (1993), 1015–1019.
[24] M.A. de Belder, L.B. Lovat, L. Tourikis, G. Leech and A. Camm, Left atrial spontaneous contrast echoes – markers of thromboembolic risk in patients with atrial fibrillation, *Eur. Heart J.* **14** (1993), 326–335.
[25] D.Y. Leung, I.W. Black, G.B. Cranney, A.P. Hopkins and W.F. Walsh, Prognostic implications of left atrial spontaneous echo contrast in nonvalvular atrial fibrillation, *J. Am. Coll. Cardiol.* **24** (1994), 755–762.
[26] E.F. Jones, P. Calafiore, J.J. McNeil, A.M. Tonkin and G.A. Donnan, Atrial fibrillation with left atrial spontaneous contrast detected by transesophageal echocardiography is a potent risk factor for stroke, *Am. J. Cardiol.* **78** (1996), 425–429.
[27] W.F. Shen, C. Tribouilloy, Z. Rida, M. Peltier, D. Choquet, J.L. Rey and J.P. Lesbre, Clinical significance of intracavitary spontaneous echo contrast in patients with dilated cardiomyopathy, *Cardiology* **87** (1996), 141–146.
[28] B.K. Shively, E.A. Gelgand and M.H. Crawford, Regional left atrial stasis during atrial fibrillation and flutter: determinants and relation to stroke, *J. Am. Coll. Cardiol.* **27** (1996), 1722–1729.
[29] T. Kallio, A. Alanen and M. Kormano, The in vitro echogenicity of flowing blood in patients with vascular disease and the effect of naftidrofuryl, *Ultrasound Med. Biol.* **15** (1989), 555–559.
[30] R.S. Finkelhor, W.E. Lamont, S.K. Ramanavarapu and R.C. Bahler, Spontaneous echocardiographic contrast in the thoracic aorta: factors associated with its occurrence and its association with embolic events, *Am. Heart J.* **130** (1995), 1254–1258.
[31] M.M. Dauzat, J.P. Laroche, C. Charras, B. Blin, M.M. Domingo-Faye, P. Sainte-Luce, A. Domergue, F.M. Lopez and C. Janbon, Real-time b-mode ultrasonography for better specificity in the noninvasive diagnosis of deep venous thrombosis, *J. Ultrasound Med.* **5** (1986), 625–631.
[32] U. Haberkorn, I. Zuna, A. Lorenz, H. Zerban, G. Layer, G. van Kaick and U. Rath, Echographic tissue characterization in diffuse parenchymal liver disease: correlation of image structure with histology, *Ultrason. Imaging* **12** (1990), 155–170.
[33] Y.M. Kadah, A.A. Farag, J.M. Zurada, A.M. Badawi and A.M. Youssef, Classification algorithms for quantitative tissue characterization of diffuse liver disease from ultrasound images, *IEEE Trans. Med. Imaging* **15** (1996), 466–478.
[34] O. Basset, Z. Sun, J.L. Mestas and G. Gimenez, Texture analysis of ultrasonic images of the prostate by means of co-occurrence matrices, *Ultrason. Imaging* **15** (1993), 218–237.

[35] F.M. Valckx and J.M. Thijssen, Characterization of echographic image texture by cooccurrence matrix parameters, *Ultrasound Med. Biol.* **23** (1997), 559–571.
[36] J.M. Thijssen, B.J. Oosterveld, P.C. Hartman and G.J. Rosenbusch, Correlations between acoustic and texture parameters from RF and B-mode liver echograms, *Ultrasound Med. Biol.* **19** (1993), 13–20.
[37] W.H. Hosmer and S. Lemeshow, *Applied Logistic Regression*, John Wiley & Sons, New York, 1989.
[38] D. Fatkin, T. Loupas, J. Low and M. Feneley, Inhibition of red cell aggregation prevents spontaneous echocardiographic contrast formation in human blood, *Circulation* **96** (1997), 889–896.
[39] H. Kitamura and S. Kawasaki, Detection and clinical significance of red cell aggregation in the human subcutaneous vein using a high-frequency transducer (10 MHz): a preliminary report, *Ultrasound Med. Biol.* **23** (1997), 933–938.
[40] G. Cloutier and Z. Qin, Ultrasound backscattering from non-aggregating and aggregating erythrocytes – a review, *Biorheology* **34** (1997), 443–470.
[41] M. Boynard and J.C. Lelievre, Size determination of red blood cell aggregates induced by dextran using ultrasound backscattering phenomenon, *Biorheology* **27** (1990), 39–46.
[42] C. Mahony, J. Ferguson and P.L. Fischer, Red cell aggregation and the echogenicity of whole blood, *Ultrasound Med. Biol.* **18** (1992), 579–586.
[43] L.Y. Mo, I.Y. Kuo, K.K. Shung, L. Ceresne and R.S. Cobbold, Ultrasound scattering from blood with hematocrits up to 100%, *IEEE Trans. Biomed. Eng.* **41** (1994), 91–95.
[44] Y.H. Lin and K.K. Shung, Ultrasonic backscattering from porcine whole blood of varying hematocrit and shear rate under pulsatile flow, *Ultrasound Med. Biol.* **25** (1999), 1151–1158.
[45] A. Sennaoui, M. Boynard and C. Pautou, Characterization of red blood cell aggregate formation using an analytical model of the ultrasonic backscattering coefficient, *IEEE Trans. Biomed. Eng.* **44** (1997), 585–591.
[46] S.Y. Kim, I.F. Miller, B. Sigel, P.M. Consigny and J. Justin, Ultrasonic evaluation of erythrocyte aggregation dynamics, *Biorheology* **26** (1989), 723–736.
[47] C. Mahony, J.L. Elion and P.L. Fischer, A computerized analysis of platelet aggregation detected by ultrasound, *Thromb. Res.* **55** (1989), 351–360.
[48] A.L. Klein, R.D. Murray, I.W. Black, S. Chandra, R.A. Grimm, D.A. DSa, D.Y. Leung, D. Miller, A.J. Morehead, S.E. Vaughn and J.D. Thomas, Integrated backscatter for quantification of left atrial spontaneous echo contrast, *J. Am. Coll. Cardiol.* **28** (1996), 222–231.
[49] G. Cloutier and Z. Qin, Shear rate dependence of ultrasound backscattering from blood samples characterized by different levels of erythrocyte aggregation, *Ann. Biomed. Eng.* **28** (2000), 399–407.
[50] G. Van Camp, B. Cosyns and J.L. Vandenbossche, Non-smoke spontaneous contrast in left atrium intensified by respiratory manoeuvres: a new transoesophageal echocardiographic observation, *Br. Heart J.* **72** (1994), 446–451.
[51] D. Fatkin, T. Loupas, N. Jacobs and M.P. Feneley, Quantification of blood echogenicity: evaluation of a semiquantitative method of grading spontaneous echo contrast, *Ultrasound Med. Biol.* **21** (1995), 1191–1198.
[52] G. Kronik, C. Stollberger, M. Schuh, F. Abzieher, J. Slany and B. Schneider, Interobserver variability in the detection of spontaneous echo contrast, left atrial thrombi, and left atrial appendage thrombi by transoesophageal echocardiography, *Br. Heart J.* **74** (1995), 80–83.
[53] A.M. Mazzone, M.P. Urbani, E. Picano, M. Paterni, E. Borgatti, A. De Fabritiis and L. Landini, In vivo ultrasonic parametric imaging of carotid atherosclerotic plaque by videodensitometric technique, *Angiology* **46** (1995), 663–672.
[54] A.D. Montauban van Swijndregt, H.R. Elbers, F.L. Moll, J. de Letter and R.G. Ackerstaff, Ultrasonographic characterization of carotid plaques, *Ultrasound Med. Biol.* **24** (1998), 489–493.
[55] J.A. Arnold, K.B. Modaresi, N. Thomas, P.R. Taylor and T.S. Padayachee, Carotid plaque characterization by duplex scanning: observer error may undermine current clinical trials, *Stroke* **30** (1999), 61–65.
[56] M. Smith-Levitin, I. Blickstein, A.A. Albrecht-Shach, R.D. Goldman, E. Gurewitsch, J. Streltzoff and F.A. Chervenak, Quantitative assessment of gray-level perception: observers' accuracy is dependent on density differences, *Ultrasound Obstet. Gynecol.* **10** (1997), 346–349.
[57] V. Uhlendorf, Physics of ultrasound contrast imaging: scattering in the linear range, *IEEE Trans. Med. Imaging* **41** (1994), 70–79.
[58] L.M. Pedro, M.M. Pedro, I. Goncalves, T.F. Carneiro, C. Balsinha, Fernandes e Fernandes and Fernandes e Fernandes, Atheroma plaque of the carotid bifurcation: how to identify an "active" lesion?, *Rev. Port. Cardiol.* **18** (1999), 699–708.
[59] M.M. Sabetai, T.J. Tegos, A.N. Nicolaides, T.S. El Atrozy, S. Dhanjil, M. Griffin, G. Belcaro and G. Geroulakos, Hemispheric symptoms and carotid plaque echomorphology, *J. Vasc. Surg.* **31** (2000), 39–49.
[60] N. el Barghouty, G. Geroulakos, A. Nicolaides, A. Androulakis and V. Bahal, Computer-assisted carotid plaque characterisation, *Eur. J. Vasc. Endovasc. Surg.* **9** (1995), 389–393.
[61] T. Elatrozy, A. Nicolaides, T. Tegos and M. Griffin, The objective characterisation of ultrasonic carotid plaque features, *Eur. J. Vasc. Endovasc. Surg.* **16** (1998), 223–230.
[62] F. Tanzi, R. Novario, L. Conte, C. Tosetto, R. Dimichele and A. Goddi, Study of ultrasonographic image textures with second-order statistical methods, *Radiol. Med. (Torino)* **97** (1999), 398–404.

[63] I. Blickstein, M. Smith-Levitin, E. Gurewitsch, J. Streltzhoff, R.D. Goldman and F.A. Chervenak, Computed sonography: requiem to echogenicity assessment?, *Gynecol. Obstet. Invest.* **44** (1997), 244–248.
[64] S. Aly and C.C. Bishop, An objective characterization of atherosclerotic lesion: an alternative method to identify unstable plaque, *Stroke* **31** (2000), 1921–1924.
[65] T.J. Tegos, M.M. Sabetai, A.N. Nicolaides, G. Pare, T.S. Elatrozy, S. Dhanjil and M. Griffin, Comparability of the ultrasonic tissue characteristics of carotid plaques, *J. Ultrasound Med.* **19** (2000), 399–407.
[66] T. Elatrozy, A. Nicolaides, T. Tegos, A.Z. Zarka, M. Griffin and M. Sabetai, The effect of B-mode ultrasonic image standardisation on the echodensity of symptomatic and asymptomatic carotid bifurcation plaques, *Int. Angiol.* **17** (1998), 179–186.